- Technical Paper -

SEISMIC EVALUATION OF A RC RIGID-FRAME ARCH BRIDGE CONSIDERING DAMAGE DUE TO EXTREME AXIAL LOAD CONDITION

Zhongqi SHI[*1], Kenji KOSA[*2], Jiandong ZHANG[*3]and Tatsuo SASAKI[*4]

ABSTRACT

Xiaoyudong Bridge received great damage in Wenchuan Earthquake. As a RC rigid-frame arch bridge, its dynamic behavior was not sufficiently studied. By 2-span dynamic analyses, it is found exposure of pile made P3 more deformable. This caused more severe local failure on Span 4, especially failure of arch leg by axial load up to 69% of N_{max}. Besides, local failure reduced degree of static indeterminacy, which caused gradual loss of entire stability. Consequently, Span 3 & 4 collapsed into river finally.

Keywords: Wenchuan Earthquake, rigid-frame arch bridge, high axial ratio, failure mechanisms

1. INTRODUCTION

Wenchuan Earthquake occurred in China, at 2:28 p.m. on May 12th, 2008. It had the magnitude of 8.0 measured by CEA and 7.9 by USGS. Report has been published saying 86 bridges suffered extensive damage or entire collapse among 1350 bridges damaged by only seismic effect in area with VII to XI seismic intensity.

Authors conducted field damage surveys of Xiaoyudong Bridge (Fig. 1), crossed Baishui River in Xiaoyudong Town on Peng-Bai Road. Based on study on rigid-frame arch bridge, it is a composite structural type of arch bridge and inclined rigid-frame bridge, and a static indeterminate structure with horizontal thrust, which has been abundantly constructed in China since 1980s. During this earthquake, two spans collapsed entirely, while another two spans stood still although severe damage can be found as well. Aiming at verifying its in-plane vibration behavior, and clarifying the possible failure mechanisms, nonlinear time-history analysis by 2-span model is conducted. Furthermore, discussion and evaluation on the failure mechanisms considering extreme axial load are conducted.

2. NONLINEAR TIME-HISTORY ANALYSIS

2.1 Analytical Modeling and Conditions

Fig. 1 shows the elevation view. Four spans (42.35m×2+43.15m×2) are arranged, numbering from left to right. Abutments and piers are also numbered from left side. Configuration of the bridge is illustrated in Fig. 2. Inclined leg and arch leg has 40° and 21° slope for each and support the girder in mid-span. Cross sections of them are shown in Fig. 2 (c) and (d). The longitudinal bar ratio and the stirrups ratio is respectively 0.97% and 0.19% for inclined leg and 1.72% and 0.16% for arch leg. Arch frame is formed by arch legs and girder in mid-span. This arch frame, together with two inclined legs and girder at the ends, compose one single rigid-frame. One span consists of five rigid-frames connected by beams, arch slab, and extending slab in transverse direction. A pier (Fig. 2 (a)) includes a RC bending frame with two columns and a beam, upon which two decks are simply supported by rubber bearings. Legs are connected to footing, which is supported by RC piles.

The damage condition of collapsed Span 3 & 4 is summarized in Fig. 3. It can be found that girder dropt totally, with all legs destroyed. Besides, P3 tilted towards A2 side for about 7.5º (also see Fig. 4).

The 2-span models are made for Span 3 & 4 to verify its possible failure mechanisms and the vibration behavior. As shown in Fig. 3, noticing five arch frames on transversal direction, we select one single arch frame, including slab, to establish 2D model. The pile beneath P3 has been exposed before Wenchuan Earthquake probably due to scouring, which is a special character of Span 3 & 4distinguished from Span 1 & 2. Aiming at taking the damage of pile beneath P3 into consideration, tri-linear M-Φ model is set for it, to simulate the exposure of it before the occurring of earthquake. Rigid elements have been set to the following parts: the

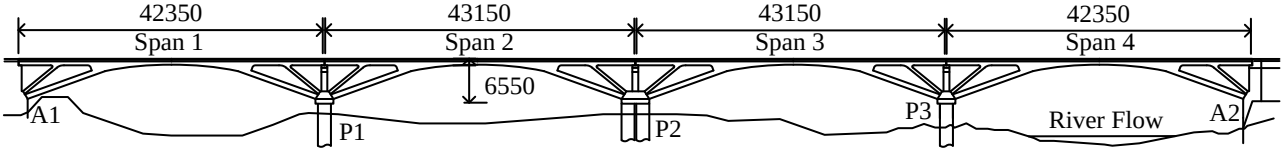

Fig. 1 Elevation View of Xiaoyudong Bridge (unit: mm)

*1 Ph.D. Candidate, Graduate School of Engineering, Kyushu Institute of Technology, JCI Student Member
*2 Ph.D., Prof., Department of Civil Engineering, Kyushu Institute of Technology, JCI Member
*3 Senior Engineer, Jiangsu Transportation Research Institute, China, JCI Member
*4 Manager, Technical Generalization Division, Nippon Engineering Consultants Co., Ltd., JCI Member

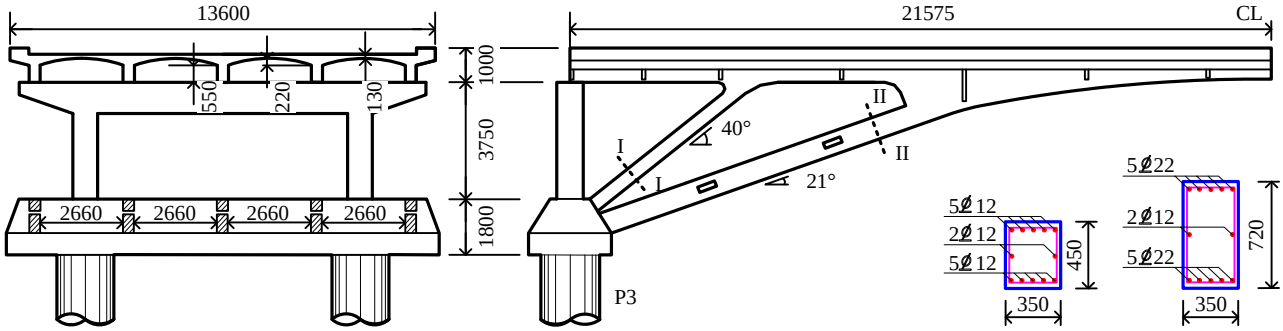

(a) Cross section view (b) Elevation view (left half of Span 4) (c) Section I−I (d) Section II-II

Fig. 2 Configuration of Xiaoyudong Bridge (unit: mm)

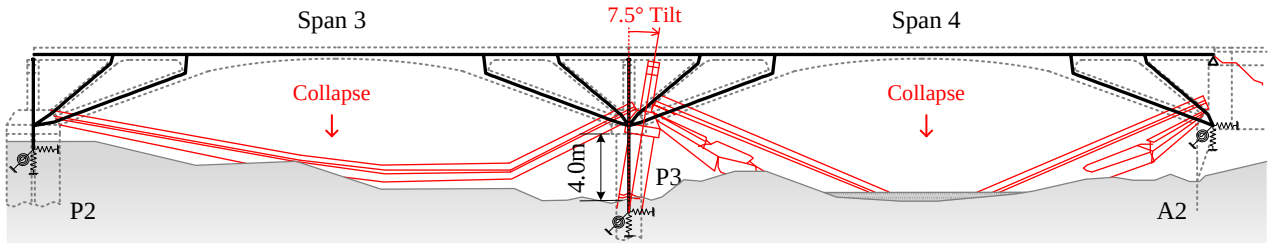

Fig. 3 Analytical model for Span 3 & 4 (view from upstream)

footing, the beam on the top of the piers and the joints between legs and girder. Tri-linear M-Φ elements calculated based on Specification for Highway Bridges (Part V Seismic Design) are used for other parts. Then, M-Φ relationships are calculated considering axial forces when only dead load acts on the structure. Under this condition, the axial load in section of Arch Legs is about 24% of its axial compressive resistance. Here, Hoshikuma equation and bi-linear stress-strain relation is applied to concrete and reinforcement respectively. Besides, vertical, horizontal and rotational springs are set under piers and abutments. For springs between girder and pier, a comparatively weak frictional spring and a supporting spring are used on pier. On the other hand, frictional and supporting springs are used on top of abutment. Collision spring is not taken into account. In actual, shear failure was not able to be confirmed except for legs on A1 probably due to collision with revetment. In analysis, peak shear response reaches only 17% of the shear resistance. Thus, evaluation is mainly conducted based on flexure, ignoring shear.

Thanks to the closest distance from Xiaoyudong Bridge of 24 km, Bajiao wave is used in analysis. For the damping, 20% is used for springs at basement, while 2% is used for all other concrete members. Rayleigh damping by eigen-vibration analysis is applied for entire structure. For calculation, Newmark-β (β= 1/4) method is applied in the numerical integration with the time step being 1/1000s.

2.2 General Results

Evaluation will be explained for Span 4 as representative, for flexure as reason stated above. The entire deformation shape at 41.35s, when mid-span of girder reaches the maximum horizontal displacement is shown in Fig. 5 (a). Besides, response curvature (Φ_t) at time point t (41.35s, when girder reaches maximum

Fig. 4 Damage of P3 (view from downstream)

horizontal displacement) and peak response curvature (Φ_{max}) are illustrated in Fig. 5, (b) for left arch leg, (c) for girder at mid-span and (d) for right arch leg.

For the deformation shown in Fig. 5 (a), the most distinctive phenomenon is the noticeably deformed P3 (3.77cm at footing). Since this great movement of P3 towards A2 side, the span is shortened, and deformation develops obviously. Point D (joint between girder and right arch leg) moves 3.65cm towards right and 7.88cm upwards, while Point C (joint between girder and left arch leg) moves almost horizontally for 3.73cm towards right. From the curvature distribution shown in Fig. 5 (b~d), it can be confirmed that the girder joints with arch legs suffer the greatest response. Respectively 1.20 and 0.54 times of the ultimate curvature (Φ_u) can be found at this time point (41.35s) for the right and the left side. For the peak response, both sides exceed the ultimate stage with 1.24 and 1.10 times of ultimate curvature respectively. For the arch legs, greater value of 0.45 times of the ultimate curvature (Φ_u) can be observed at the bottom of right arch leg (connecting to

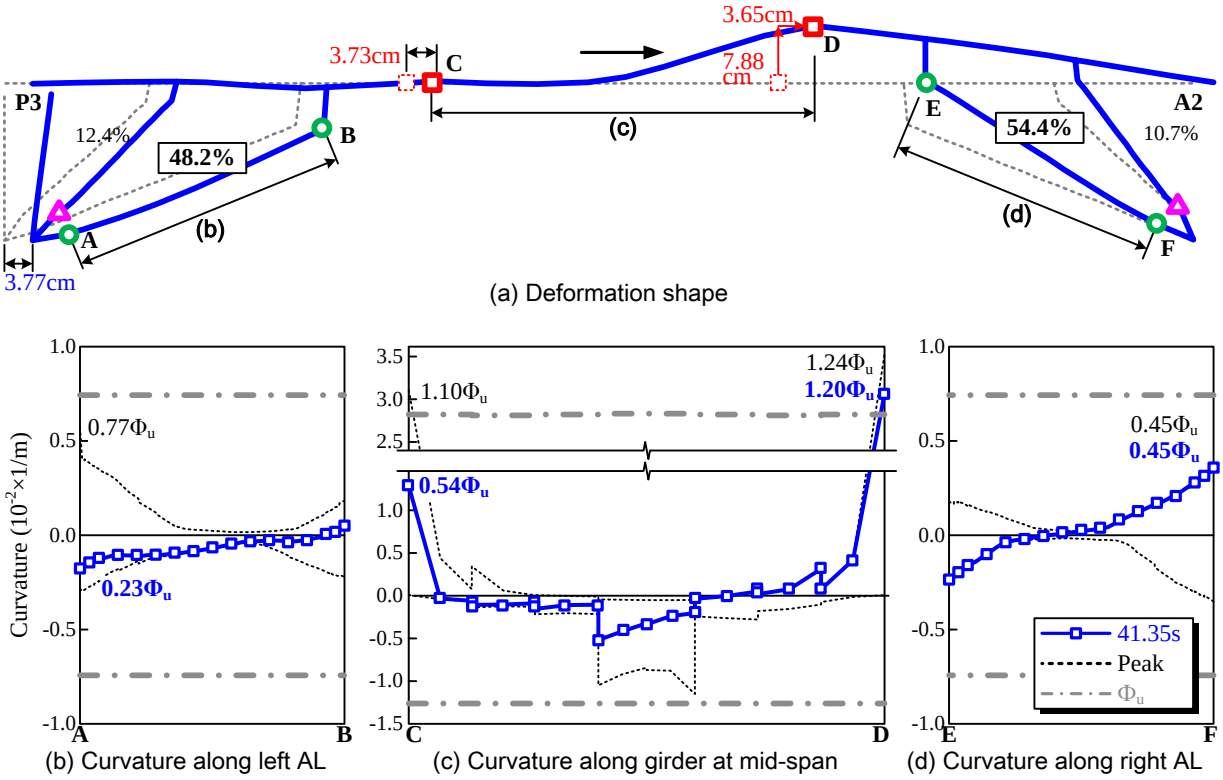

Fig. 5 Analytical result of Span 4 at 41.35s (peak displacement) and at maximum response

A2), while the bottom of left arch leg (connecting to P3) reaches only 0.23 Φ_u. The peak response occurs at this time point for the right arch leg, while it becomes greater (0.77 Φ_u) for the left arch leg although the ultimate stage is not reached yet. However, it should be specially noticed that significant axial ratio (48.2% for left and 54.4% for right) can be found for the arch legs, probably due to the enormous movement of P3.

As a result, the summary of failure of Span 4 by compared the peak response curvature (Φ_{max}) with the ultimate curvature (Φ_u) is shown in Fig. 6. Here, zone (a) means the peak response curvature exceeds the ultimate curvature and the member vibrates beyond the ultimate stage; zone (b) suggests the member does not reach the ultimate stage yet. As a consequence, notable damage (beyond the ultimate stage) is able to be observed at girder joints with arch legs, and at bottom of inclined legs. The flexural response at bottom of arch legs does not reach the ultimate stage.

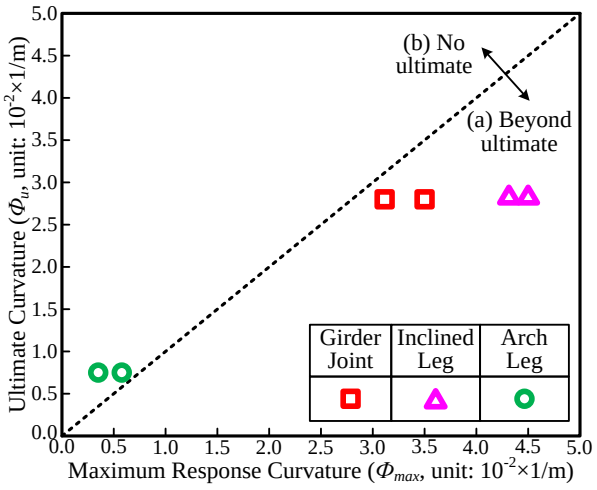

Fig. 6 Summary of failure on Span 4

3. FAILURE OF LEGS BY HIGH AXIAL LOAD

The general analytical results were explained. Although bottom of arch legs did not reach its ultimate stage, the axial response was found relatively obvious. In this chapter, the detailed analytical result of arch legs will be explained concentrating on the axial loads, followed by discussion on the failure judged by other experimental tests.

3.1 Analytical Response of Arch Leg

As mentioned in Section 2.2, axial response was found notable for arch legs of Span 4 based on dynamic analysis. Fig. 7 illustrated the response range of M-N

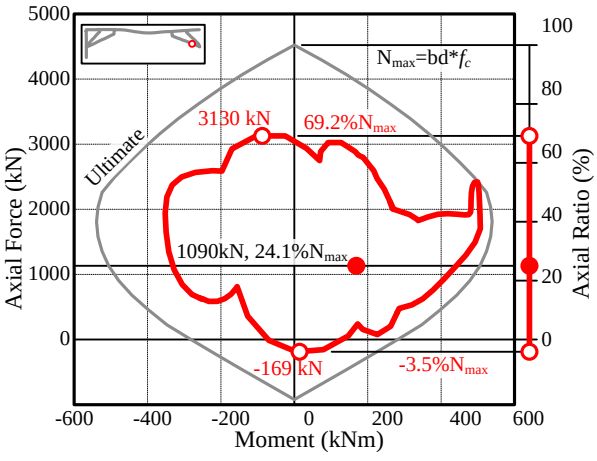

Fig. 7 Response M-N history

history at bottom of right arch leg of Span 4, as well as the axial ratio of it. Here, N_{max} ($=bd*f_c$) is defined as maximum axial resistance. It can be observed that the bottom of arch leg responses significantly in both flexural direction and axial direction. The axial load has already exceeded the peak point, and reached 3130 kN for the maximum value, suggesting the axial ratio reaches 69.2% of N_{max}. This phenomenon may probably influence the failure of arch leg significantly.

To explain the occurrence of axial load in cross section of arch leg, the mechanisms is drawn in Fig. 8 for the right half of Span 4, and the comparison of axial load in different members between the peak response axial load and that under only dead load for Span 4 is plotted in Fig. 9 (here, the shear force in legs and bearing resistance at girder end are ignored, since the values are relatively small). As shown in Fig. 8, when girder moves towards right side (A2 for Span 4) under the effect of horizontal load (F_H) acting on girder, axial load will be transmitted to arch leg and inclined leg. The resistance, therefore, occurs at bottom of them (F_A by arch leg, and F_I by inclined leg). Because of smaller angle of 21° to the horizon, arch leg may resist more from girder, leading to greater resistance F_A. With greater angle of 40°, the inclined leg may not be able to resist the load from girder by axial load (F_I), although the flexural response may occur notably. Besides, when mid-span moves downwards, arch leg is compressed to be shorter, which causes extra axial load occurred in cross section of arch leg. The peak response axial loads in girder, arch leg and inclined leg connected to A2 on Span 4 are plotted compared with that under only dead load in Fig. 9, to explain the mechanisms in Fig. 8. It can be observed that the axial load in girder at mid-span increases from 1580 kN under only dead load by 73% to maximum 2730 kN, and the axial load in inclined leg rises from 430 kN under only dead load by 121% to maximum 950 kN. On the other hand, axial load in arch leg increases significantly from 1090 kN (24.1% of N_{max}) under only dead load to maximum 3130 kN (69.2% of N_{max}). The increasing ratio is as great as 187%. It can be inferred that by great seismic effect, axial load vibrates noticeably for both the legs. Especially, arch leg suffers extremely high axial load (3130 kN, 69.2% of N_{max}), which is about 3.3 times of the peak axial load (950 kN) of inclined leg.

To sum it up, arch leg is a main supporting member where great axial response is easy to happen due to small angle to the horizon. Extremely high axial load (69.2% of N_{max}) is very likely to occur in arch leg.

3.2 Experimental Behavior of RC Column under High Axial Load

To assess the possible failure of arch leg under high axial load, experimental tests on axial loaded RC column were selected in the database[1] for ASCE/SEI 41-06 standard and all proceedings of JCI. Therefore, totally about 400 rectangular columns have been studied. Here, considering configurations of arch leg, following assumptions are used in the selection for the comparison with analytical result: (1) failure mainly by flexure; (2) cantilever type RC column; (3) normal

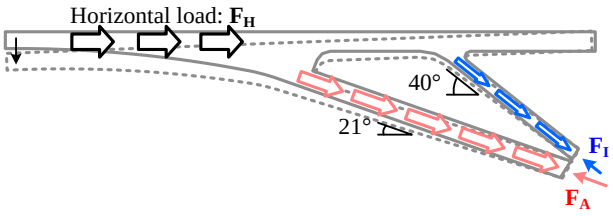

Fig. 8 Mechanisms of axial load transmission

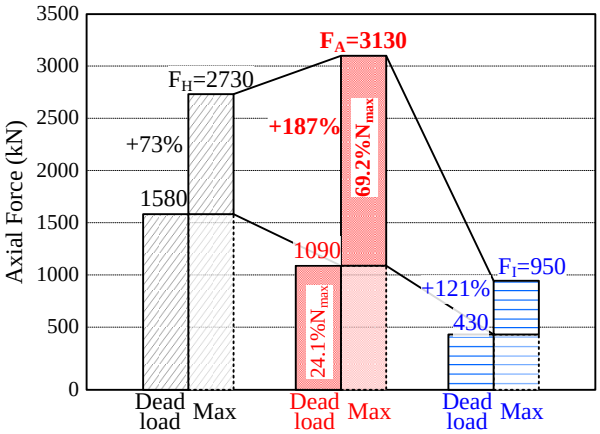

Fig. 9 Comparison of axial load in different members

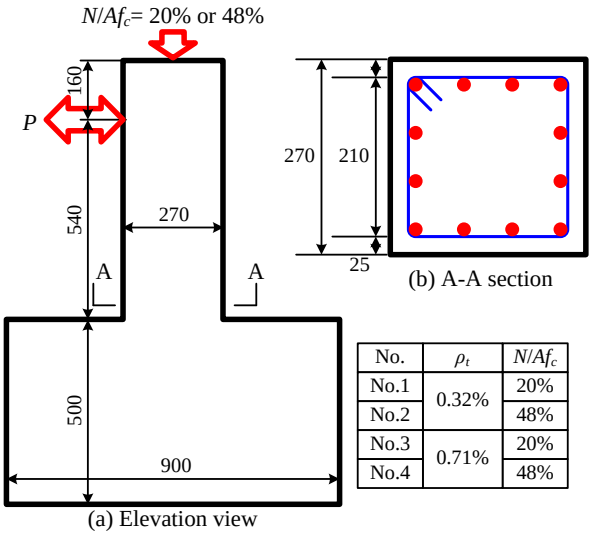

No.	ρ_t	N/Af_c
No.1	0.32%	20%
No.2		48%
No.3	0.71%	20%
No.4		48%

Fig. 10 Experimental setup based on reference[2]

concrete strength (f_c no greater than 50 N/mm^2); (4) low tie ratio (volume ratio, not greater than 1.0%); and (5) high axial ratio (maximum value greater than 40%).

Configuration of the typical selected specimens[2] is shown in Fig. 10. In this series of experimental tests, cyclic lateral load was acted on 4 specimens with 2 types of ties (0.32% and 0.71%), under 2 levels of axial ratio (20% and 48%). Therefore, the influence on ductility of RC column by ties ratio and axial ratio can be evaluated. In the experimental test, lateral displacement at loading height was measured, and the representative results, the envelops of P-δ history for the low ties ratio series (0.32%), are illustrated in Fig. 11. The black solid line shows the one under 20% axial

ratio, in which the lateral resistance dropped gradually after the peak. On the other hand, the red dot line stands for the one under 48% axial ratio, showing very dramatic drop of lateral resistance after the peak. Then, by defining the ultimate stage as when lateral load drops to 80% of the maximum resistance, the ultimate displacement (δ_u) can be got. With smaller axial ratio (20%), No. 1 specimen reaches its ultimate stage at 1.53cm. However, with greater axial ratio (48%), No. 2 specimen reaches its ultimate stage earlier at 0.75cm, which is 49.0% of that for No. 1 specimen. Further, relation between ultimate displacement and axial ratio is summarized in Fig. 12 based on these experimental tests. For two series of specimen with different ties ratio (0.32% and 0.71%), obvious drop of ultimate displacement can be observed. Ultimate displacement decreased from 17.7mm with 0.71% ties ratio by 13.6% to 15.3mm with 0.32% at low axial ratio (20%), while it decreased from 11.1mm with 0.71% ties ratio by 31.5% to 7.6mm with 0.32% at high axial ratio (48%). It can be inferred that ultimate displacement is expected to drop especially under high axial ratio (48%), due to weakened confinement effect when the ties ratio changes from 0.71% to 0.32%. On the other hand, displacement decreased by 37.3% with 0.71% ties ratio (from 17.7mm to 11.1mm), and by 50.3% with 0.32% ties ratio (from 15.3mm to 7.6mm). This indicates that ultimate displacement may drop greatly when axial ratio increases from 20% to 48%. This phenomenon is more obvious in specimen with low ties ratio (0.32%). As been shown in Fig. 11, with 0.32% ties ratio, two specimens had similar displacement for the peak points with different axial ratio, but the lateral load is greater under 48% axial ratio since the longitudinal bars became more difficult to yield due to high compressive load. However, ultimate displacement distinguished from each other notably. For low axial ratio (20%), compressive load of concrete has not developed greatly at yield, thus the lateral load drops gradually and the ultimate stage is reached slowly. For high axial ratio (48%), special attention should be paid that probably because the concrete at base already suffers great compressive stress and strain at when longitudinal bar reaches yield, the lateral load decreases dramatically and the ultimate stage (at 80% of P_{max}) is reached very soon. This causes the significant drop of ultimate displacement especially with low ties ratio.

3.3 Failure of Arch Legs

Besides, specimens are calculated ignoring slip of reinforcement and shear deformation for simple, by using Hoshikuma equation[3] for concrete (considering its good applicability for member to low stirrups ratio) and bi-linear stress-strain relation for reinforcement. Calculation example (No. 2: axial ratio of 48% and stirrups ratio of 0.32%) is shown in Fig. 13 ((a) for moment, (b) for curvature and (c) for deformation). After calculating moment and curvature at yield and ultimate ($M'_{y\text{-}2}$ and $M'_{u\text{-}2}$, $\Phi'_{y\text{-}2}$ and $\Phi'_{u\text{-}2}$, apostrophes suggest the calculated result), curvature distribution can be got (Fig. 13 (b)). Assumption of triangle curvature distribution is used here since the plastic hinge length is

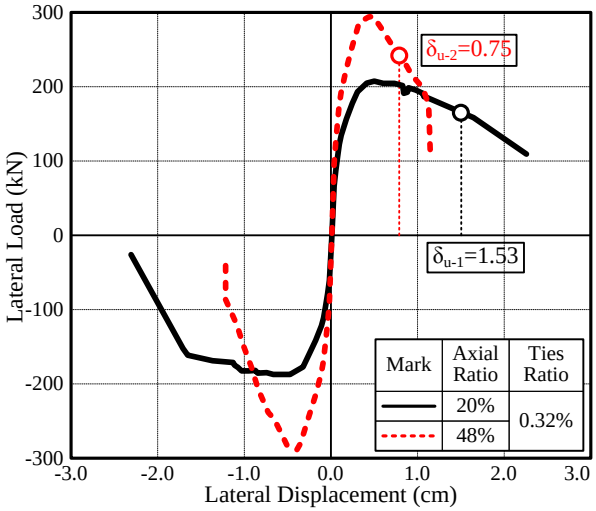

Fig. 11 Experimental P-δ curves (No. 1 VS No. 2)

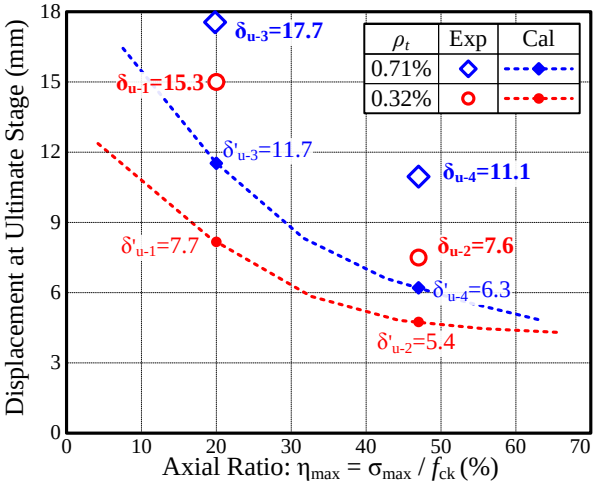

Fig. 12 Relation between ultimate displacement VS axial load

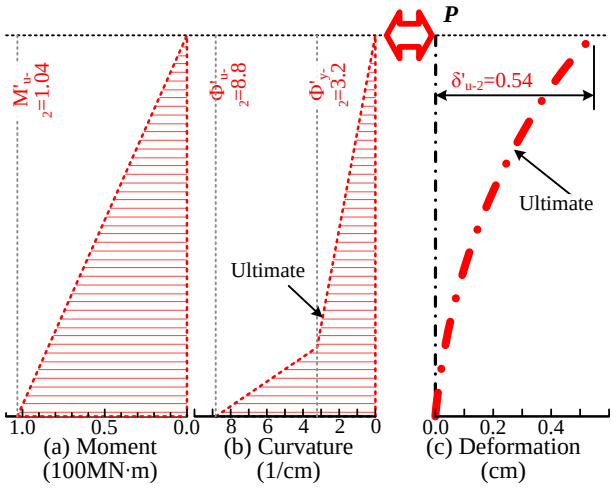

Fig. 13 Calculation of flexural deformation (No. 2: axial ratio: 48%; stirrups ratio: 0.32%)

complex to determine. Then, by integrating curvature along height till the loading point, the ultimate displacement ($\delta'_{u\text{-}2}$) can be got. Therefore, the ultimate displacements for two kinds of stirrups ratio, and under different axial ratios are calculated, and compared with experimental results in Fig. 12. As shown, although calculated result of ultimate displacement is generally smaller than experimental results (probably because of ignore of slip and shear), decreases of ultimate displacement due to both stirrups ratio drop and axial ratio increase is reappeared well. It indicates that the flexural deformation was calculated accurately.

Then the result of ultimate curvature is shown in Fig. 14 compared with analytical result of arch leg. Calculated ultimate curvature curves are plotted for stirrups ratio of 0.19% for arch leg of Xiaoyudong Bridge. Although the analytical result shows that the peak response curvature of arch leg (0.57×10^{-2} 1/m and 0.35×10^{-2} 1/m for left and right arch leg on Span 4) does not exceed the ultimate curvature (0.74×10^{-2} 1/m) calculated with axial ratio (24.1%) when subjected to only dead load, severe damage can be expected since they locates above the ultimate curvature curves if taking the increase of axial ratio into account. This suggests that by extremely high axial load (axial ratio being 69.2% and 50.0%), and very low stirrups ratio (0.19%), there is considerable probability for bottom of both arch legs on Span 4 to suffer severe damage, leading to capacity loss.

4. POSSIBLE FAILURE MECHANISMS

For failure mechanisms, simplified 1/2-span mechanical model is used for explanation, using Degree of Static Indeterminate (DSI in following). As a rigid -frame structure, we can get DSI of this model is 6 at initial stage. Capacity in all three directions is supposed to be ignored, which indicates that DSI will decrease by 3 with one ultimate stage of local member. As shown in Fig. 15 (a), because of the ultimate stages at Point a and b, structural DSI will increase from 6 to 0, indicating that structure becomes static determinate and any further local failure and loss of DSI will result in entire failure of structure. Therefore, possible failure at Point c due to extremely high axial load and low stirrups ratio will destroy the structure and cause collapse as shown in Fig. 15 (b). From another point of view, ultimate stages at Point a and b (in Fig. 15 (a)) will isolate arch leg from being connected with girder and inclined leg, and make arch leg a cantilever-like system. Then, due to possible ultimate stage of Point c, clock-wise rotation (Fig. 15 (b)) will occur on this cantilever-like system. As a result, Span 4 probably collapsed entirely.

5. CONCLUSIONS

Analytical results were summarized based on dynamic analysis by 2-span model, and the possible failure mechanisms were verified after assessing the further failure of local member under extreme axial load condition, following conclusions have been drawn:

(1) By dynamic analysis, girder joints with arch leg may suffer ultimate stage. However, pile exposure induced notable vibration of P3 and caused severe failure at bottoms of legs on Span 4. Thus, both inclined legs on Span 4 suffered ultimate stage.

(2) Besides, due to the drop of ultimate displacement caused by high axial ratio and low stirrups ratio, severe damage might also occur to arch legs on Span 4, demonstrated based on experimental result. Thus, together with the ultimate stage at girder joints, and bottoms of inclined leg, Span 4 would lose its entity and collapsed totally.

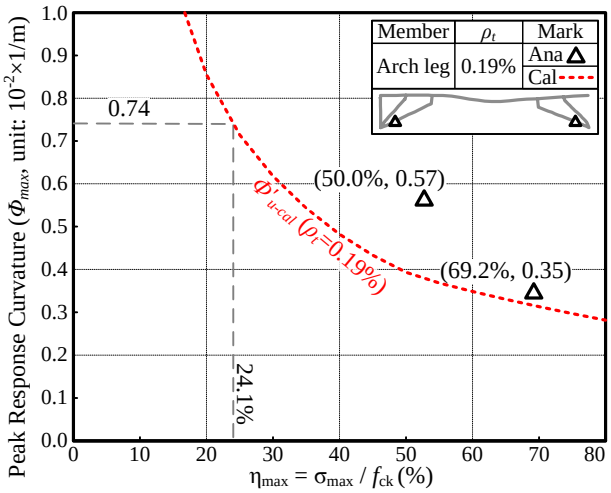

Fig. 14 Axial ratio-plastic ratio relation of arch leg

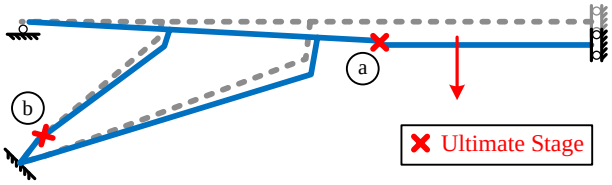

(a) Ultimate Stages of Point a and b

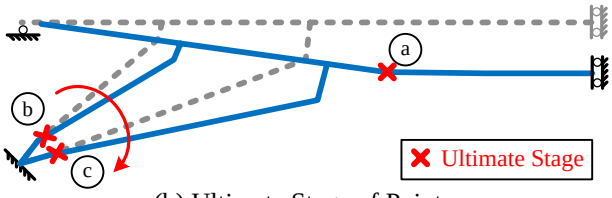

(b) Ultimate Stage of Point c

Fig. 15 Possible failure mechanisms for Span 4

REFERENCES

[1] Balaji Sivaramakrishnan, "Non-Linear Modeling Parameters for Reinforced Concrete Columns Subjected to Seismic Loads", Master Thesis, Univ. of Texas at Austin, 2010

[2] Yasutomi, Y. et al., "Quantitative Evaluation of Residual Crack for RC Column under Certain Axial Load", Proc. of JCI, Vol. 27, No. 2, 2005, pp. 259-264 (in Japanese)

[3] Hoshikuma, J. et al., "A Stress-Strain Model for Reinforced Concrete Columns Confined by Lateral Reinforcement", Journal of JSCE, No.520/V-28, 1995, pp. 1-11 (in Japanese)